^{18}F-FDG PET Study Reveals Brain Functional Changes During Attention in Rats

Wang Xi[1–4], Danting Su[5], Binbin Nie[6], Yanqin Yu[7], Baoci Shan[6], Qiaozhen Chen[1–4], Mei Tian[1–4], and Hong Zhang[1–4]

[1]Department of Nuclear Medicine, The Second Affiliated Hospital of Zhejiang University School of Medicine, Hangzhou, China; [2]Zhejiang University Medical PET Center, Hangzhou, China; [3]Institute of Nuclear Medicine and Molecular Imaging of Zhejiang University, Hangzhou, China; [4]Key Laboratory of Medical Molecular Imaging of Zhejiang Province, Hangzhou, China; [5]Zhejiang Provincial Center for Disease Prevention and Control, Hangzhou, China; [6]Key Laboratory of Nuclear Analytical Techniques, Institute of High Energy Physics, Chinese Academy of Sciences, Beijing, China; and [7]Department of Neurobiology, Key Laboratory of Medical Neurobiology of Ministry of Health and Zhejiang Province, Key Laboratory of Neurobiology, Zhejiang University School of Medicine, Hangzhou, China

Attentional impairments are seen in many clinical syndromes, including attention deficit hyperactivity disorder, schizophrenia, and Alzheimer disease. Understanding the mechanism of attention can be helpful for the diagnosis and treatment of these diseases. The aim of this study was to assess brain glucose metabolic changes in a rat model of attention. **Methods:** Small-animal PET studies were performed at 4 stages. Statistical parametric mapping was used for image analysis. **Results:** Increased ^{18}F-FDG uptake was found in the lateral hypothalamic area and left accumbens nucleus in the learning condition. Under the attentive condition, increased ^{18}F-FDG uptake was observed in the right retrosplenial cortex but ^{18}F-FDG uptake was decreased in the right medial geniculate nucleus. ^{18}F-FDG uptake change in the right retrosplenial cortex was negatively correlated with correct latency of behavior performance. **Conclusion:** ^{18}F-FDG small-animal PET imaging provided novel findings on attention-related glucose metabolic changes, which were significantly correlated with the behavior performance in this rat model.

Key Words: positron emission tomography (PET); ^{18}F-FDG; neurology; attention; rat model

J Nucl Med 2013; 54:1969–1973
DOI: 10.2967/jnumed.113.123000

The conscious experience of directing attention to an external event or an internal thought is one of the mysterious areas in neuroscience. Attentional impairments are seen in many clinical syndromes, including attention deficit hyperactivity disorder (*1*), schizophrenia (*2*), and Alzheimer disease (*3*). Understanding the mechanism of attention can be helpful for the diagnosis and treatment of these diseases.

Received Mar. 12, 2013; revision accepted Jun. 25, 2013.
For correspondence or reprints contact either of the following:
Mei Tian, Department of Nuclear Medicine, The Second Affiliated Hospital of Zhejiang University, 88 Jiefang Rd., Hangzhou, Zhejiang 310009, China.
E-mail: meitian@gmail.com
Hong Zhang, Department of Nuclear Medicine, The Second Affiliated Hospital of Zhejiang University, 88 Jiefang Rd., Hangzhou, Zhejiang 310009, China.
E-mail: hzhang21@gmail.com
Published online Oct. 10, 2013.

Over the past century, considerable studies have taken effort to reveal the neural circuits in the attention behavior using a wide variety of paradigms and models. Although neuropharmacology and lesion studies have provided preliminary knowledge about the neural network basis of attention, little is known about regional neuronal activity changes associated with attention in living subjects because of the unacceptable trauma of microdialysis and biopsy procedures. Therefore, a noninvasive functional imaging approach for visualization and quantification of brain functional changes is urgently needed.

Recently, ^{18}F-FDG PET has been applied for brain regional metabolic activation, and whole-brain image analysis such as statistical parametric mapping has been applied to enable relating measured behavior to brain metabolic changes in humans (*2,4*) and rodents more extensively (*5,6*). However, to our knowledge, there was no evidence of in vivo functional imaging of behavioral attention tasks in rodents. The aim of this study was to use ^{18}F-FDG uptake, an index of neuronal activity, to measure brain glucose metabolism changes during attention tasks in a series of small-animal PET studies and to study the relationship between the regional brain activity and behavioral output in a rat model of attention.

MATERIALS AND METHODS

Animals

Twelve adult male test-naïve Sprague–Dawley rats were used for this study. All animal experiments were performed with the approval of the Institutional Animal Care and Use Committee (details are provided in the supplemental materials, available at http://jnm.snmjournals.org).

Apparatus and Behavior Task

Behavior experiments were conducted using the visual-guided 5-choice serial reaction time task (5-CSRTT) in a 5-hole operant chamber (25 × 25 × 25 cm; Anilab Software & Instruments Co., Ltd.) within a sound-attenuating small dark room as described previously (*7,8*). At stage 0, rats were trained to correlate the light hole with the sucrose solution reward, in which all of the 5-hole lights turned on until the rat's nose poked into one of the light holes and the reward of sucrose solution was given at the food well (Fig. 1B; Supplemental Movie 1). After that, rats were trained in 12 successive standard stages (1–12) (details are provided in the supplemental materials).

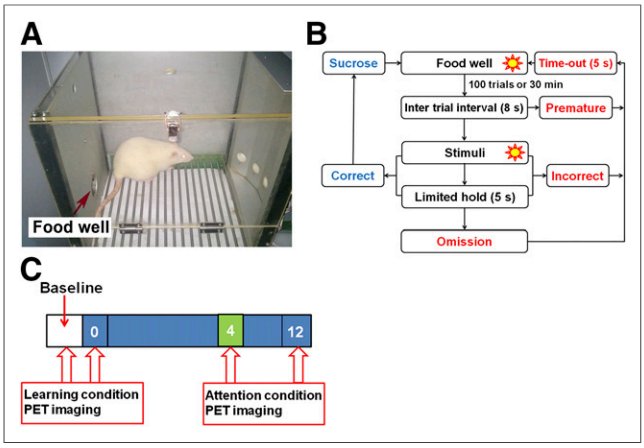

FIGURE 1. Schematics of 5-CSRTT and ^{18}F-FDG small-animal PET imaging protocols. (A) Representative photo of 5-hole operant chamber. (B) Training session included 100 trials or lasted for 30 min. After 8-s intertrial interval, 1 of 5 holes was randomly illuminated for 0.5 s. If rat made premature nose poke before light illumination, light was extinguished for 5 s and then new trial was started. Rat had 5 s to respond into one of the holes. A correct response led to reward delivery into food well on wall opposite holes. Incorrect response or omission of response led to light off. After error, a new trial was begun, and light was illuminated again after rat poked its nose into empty food magazine. (C) ^{18}F-FDG small-animal PET imaging protocols. ^{18}F-FDG small-animal PET studies were done at baseline and stage 0 for learning condition, then at stage 4 and stage 12 for attention condition.

Small-Animal PET Imaging Protocols

Immediately after intraperitoneal injection of ^{18}F-FDG (62.9–77.7 MBq), each rat performed attentive behavior for 30 min, and then rats were anesthetized with isoflurane (2%) and fixed in the microPET R4 scanner (Siemens Medical Solutions). PET imaging was acquired at 40 min after ^{18}F-FDG injection (details are provided in the supplemental materials).

Image Analysis and Statistics

Image analysis was performed using an improved toolbox for voxelwise analysis of rat brain images based on SPM8 (Welcome Department of Cognitive Neurology) (*9*). One-way repeated-measures ANOVA were used to analyze behavior performance parameters, and Pearson correlation was used to examine correlation between ^{18}F-FDG uptake and behavior performance parameters. Data were given as mean ± SEM. All statistical analyses of behavior and correlation were performed using SPSS software (version 11.0; SPSS Inc.). The level of statistical significance was set at a P value of less than 0.05.

RESULTS

5-CSRTT Behavior and Performance

In this study, 8 of 12 rats reached the performance criteria from stage 1 (30-s light duration) to stage 12 (0.5-s light duration) after about 50 training days (Fig. 2; Supplemental Movies 1–4). At stage 12, the accuracy of behavior performance was 89.1% ± 1.3%; of premature responses, 7.8 ± 2.0; and of omissions, 8.4 ± 0.9. An additional 20 training sessions were performed after rats met the stage-12 criteria to ensure they were in a stable condition. The accuracy of each session is summarized in Figure 2D. An accuracy of greater than 80% was considered stable.

Behavior Performance and ^{18}F-FDG Small-Animal PET Imaging in Learning Condition

Compared with the baseline state, more food rewards could be reached by rats at stage 0. There was significant difference of food intake between baseline and stage 0 (4.75 ± 1.5 vs. 100 ± 0, $P < 0.05$; Supplemental Fig. 1, Supplemental Movies 1 and 2). A significantly increased or decreased ^{18}F-FDG uptake associated with the conditional learning process is summarized in Table 1. Representative images are shown in Supplemental Figure 2.

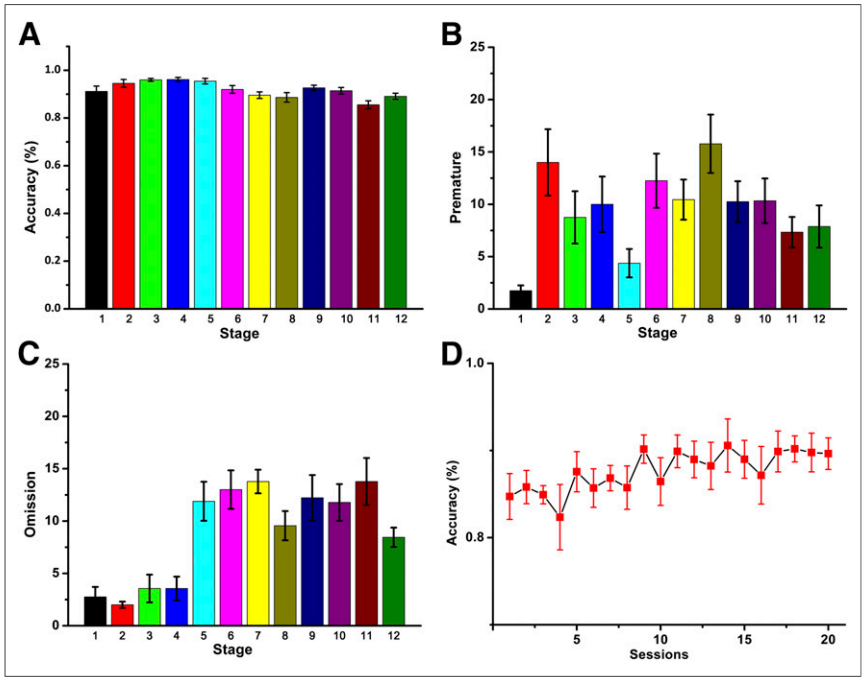

FIGURE 2. Attentive behavior performance. Rats were trained in 5-CSRTT using gradual decreased stimuli duration from 30 to 0.5 s in 12 stages. Performance criteria were used to justify whether rats were qualified for next level. (A) Accuracy (a parameter of attention) of each stage. (B) Number of premature response in each stage. (C) Number of omission in each stage. (D) Accuracy for 20 sessions (0.5-s light duration) after rats met stage 12 performance criteria. Error bars indicate SEM.

Behavior Performance and ^{18}F-FDG Small-Animal PET Imaging in Attentive Condition

To ensure rats were in a stable condition at stage 12, ^{18}F-FDG small-animal PET studies were performed after an additional 20 training sessions as described in the "Materials and Methods" section. The accuracies of stage 4 (less-attentive condition) and stage 12 (extensive-attentive condition) were 96.9% ± 0.4% and 91.4% ± 1.4%, respectively. Correct trials were similar between stage 4 and stage 12 (68.3 ± 0.8 and 73.4 ± 4.0, respectively, $F[1,14] = 1.59$, $P > 0.05$). A significant difference was found in the correct response latency between stage 4 and stage 12 (0.931 ± 0.149 s vs. 0.557 ± 0.027 s, respectively, $F[1,14] = 6.09$, $P < 0.05$), indicating that rats responded to the visual stimuli more

TABLE 1
Significant Glucose Metabolic Changes in Learning Condition (Baseline vs. Stage 0)

Region	Coordinate (mm)			Peak level		
	x	*y*	*z*	*t* value	*z* score	$P_{uncorrected}$
Increased						
Left lateral hypothalamic area	−1	7	−2	6.08	4.03	<0.001
Left accumbens nucleus	−1	7	1	4.93	3.58	<0.001
Right lateral hypothalamic area	1	7	−2	4.76	3.50	<0.001
Left retrosplenial granular cortex	−4	4	−8	5.66	3.88	<0.001
Right cerebellum	4	6	−13	5.42	3.78	<0.001
Right medial entorhinal cortex	3	4	−9	5.27	3.72	<0.001
Left piriform cortex	−6	9	−3	5.21	3.69	<0.001
Left cingulate cortex	−1	3	2	4.81	3.52	<0.001
Right piriform cortex	5	9	−1	4.36	3.31	<0.001
Right piriform cortex	6	9	−3	4.33	3.30	<0.001
Left primary somatosensory cortex	−5	4	−3	4.28	3.27	0.001
Right accumbens nucleus	2	7	1	4.21	3.24	0.001
Decreased						
Left olfactory bulb	−1	3	7	4.84	3.54	<0.001
Right mediodorsal thalamic nucleus	1	5	−2	4.3	3.28	0.001
Left anterodorsal thalamic nucleus	−1	5	−1	4.17	3.22	0.001

quickly in stage 12 than in stage 4 (Fig. 3; Supplemental Movies 3 and 4).

When ^{18}F-FDG uptake in stage 4 and stage 12 was compared, a significant increase was found in the right retrosplenial cortex (RSC) and a significant decrease in the right medial geniculate nucleus (MGN) (Table 2; Figs. 3D and 3E). A significant negative correlation between the correct latency and interhemispheric activity difference of RSC was observed ($R = -0.505$; $P = 0.046$) (Fig. 4).

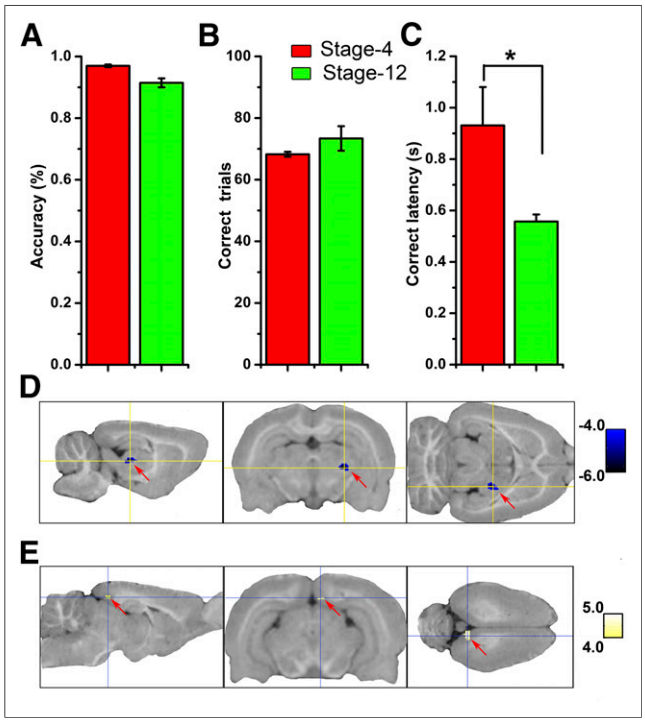

FIGURE 3. Changes of brain ^{18}F-FDG uptake from rats tested in attentive condition ($n = 6$). Accuracy (A) and correct trials (B) showed no significant difference, but correct latency (C) showed significant difference between stage 4 and stage 12 ($P < 0.05$). (D) Representative sagittal, coronal, and transverse images demonstrated decreased ^{18}F-FDG uptake in right MGN in stage 12, compared with stage 4. (E) Representative sagittal, coronal, and transverse images demonstrated increased ^{18}F-FDG uptake in RSC in stage 12, compared with stage 4. Colored bars on right express T-score levels.

DISCUSSION

In the present study, small-animal PET was used to measure ^{18}F-FDG uptake changes in the rat brain during 5-CSRTT. We found that ^{18}F-FDG uptake increased in the lateral hypothalamus, accumbens nucleus, piriform cortex, medial entorhinal cortex, left cingulate cortex, left primary somatosensory cortex, left retrosplenial granular cortex, and paramedian lobule of the right cerebellum and decreased in the olfactory bulb and thalamic nucleus region (medial-dorsal and anterodorsal parts) during the visual-guided learning condition. Furthermore, we observed that ^{18}F-FDG uptake increased in the right RSC but decreased in the right MGN, suggesting that these 2 regions were specifically involved in the extensive attention process. The negative correlation between the interhemispheric activity difference in RSC and correct latency indicate that the RSC is involved in the top-down control of extensive visual-guided attentive behavior.

This is the first, to our knowledge, in vivo imaging evidence in rodents demonstrating that the RSC is involved directly in attention behavior. In the previous lesion study, damage to the RSC in rats led to impaired spatial learning abilities. Rats failed to recall which areas of the maze they had already visited and took longer to reach the end of the maze, as compared with rats with a normal RSC (*10*). This finding is also consistent with the previous clinical functional MR imaging study demonstrating that the signal change in the posterior cingulate cortex (homologous to RSC in rats) (*11*) had a strong inverse correlation with reaction times in attentive condition (*12*). The posterior cingulate cortex also showed stronger α wave (lower frequency range of ~7–13 Hz) oscillatory activity in phonetic auditory attention in comparison to selective attention to sound locations using magnetoencephalography in humans (*13*). Pathologic changes in the posterior cingulate cortex can occur in conditions such as schizophrenia and bipolar

TABLE 2
Significant Glucose Metabolic Change in Attentive Condition (Stage 4 vs. Stage 12)

Change	Coordinate (mm)			Peak level		
	x	*y*	*z*	*t* value	*z* score	$P_{uncorrected}$
Increased						
Right RSC	1	2	−5	4.95	2.86	0.002
Right RSC	0	2	−6	4.76	2.8	0.003
Decreased						
Right MGN	3	5	−5	6.24	3.17	0.001

disorder with attention deficient syndrome (*3,14*). Interestingly, a metabolic decline region centered on the posterior cingulate cortex was found in early Alzheimer disease using ^{18}F-FDG small-animal PET (*15*).

MGN is an auditory thalamic nucleus that provides primary and immediate inputs to the auditory cortex and influences the direction and maintenance of attention (*16*). Previous functional MRI results demonstrated that attention to a single sensory modality can result in decreased activity in cortical regions that process information from an unattended sensory modality (cross-modal deactivations) (*17*). In our study, we observed that glucose metabolism increased in RSC but decreased in MGN, indicating that selective attention to visual stimuli may involve 2 separate pathways—one involved in an enhanced attended modality and another involved in neural activity suppression in areas that process input from nonattended sensory modalities (e.g., auditory system by cross-modal deactivations).

In addition, we found that during the learning condition, glucose metabolism was increased in the lateral hypothalamus, accumbens nucleus, piriform cortex, medial entorhinal cortex, left cingulate cortex, left primary somatosensory cortex, left retrosplenial granular cortex, and right cerebellum. By contrast, ^{18}F-FDG uptake was decreased in the olfactory bulb and in the medial-dorsal and anterodorsal parts of the thalamic nucleus region. These regions are associated with the complex cognitive process (including operational learning, reward, vision, and execution) during the learning process. For example, the lateral hypothalamus plays an important role on the initiation of feeding, reward, and motivation in rodents (*18,19*), and the accumbens nucleus is important in motivated, goal-directed behaviors, which was found to be related to reinforcement and reward, and actions of addictive drugs (*20*).

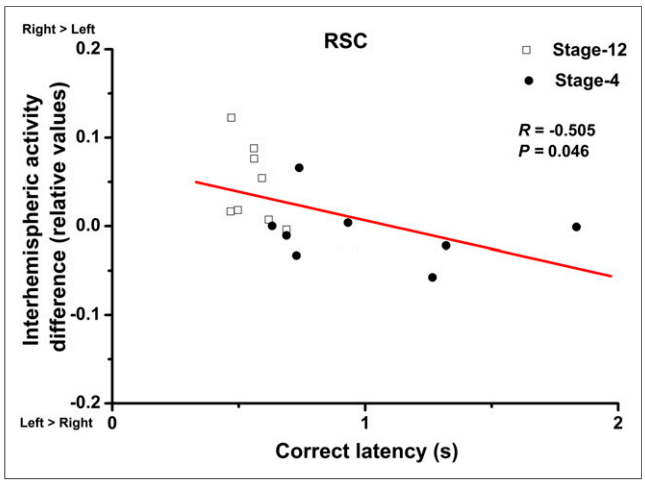

FIGURE 4. Correlation between interhemispheric activity of ^{18}F-FDG relative value and correct latency in attentive condition. Pearson correlation coefficient, $R = -0.505$, $P = 0.046$, $n = 8$.

There are some limitations in this study. First, because of the restriction of radiation exposure to each animal, ^{18}F-FDG small-animal PET studies were done at 4 different stages only (baseline, stage 0, stage 4, and stage 12). If we could perform small-animal PET scanning at all the 13 training stages, we would be able to find out the temporal dynamics of glucose metabolic changes during the attentive training sessions. Second, although the self-controlled comparison was used in this study, an additional age-comparable, nontraining (naïve) control group should be used in the further study, to avoid the influence of environmental familiarity to the animal during the 3-mo training period. Third, ^{18}F-FDG small-animal PET imaging was the only imaging modality used in this study. Multimodality imaging combined with electrophysiologic techniques and pathologic staining could provide more detailed information on structure, function, and neurophysiobiology. On the basis of the findings from this study, we will continue the further research to find the optimal approach for the diagnosis and treatment of attention-associated diseases.

CONCLUSION

^{18}F-FDG small-animal PET imaging provided novel findings on attention-associated glucose metabolic changes, which were significantly correlated with the behavior performance in this rat model of attention. ^{18}F-FDG PET imaging can be a potential approach for noninvasive diagnosis and therapeutic evaluation of attention-related diseases.

DISCLOSURE

The costs of publication of this article were defrayed in part by the payment of page charges. Therefore, and solely to indicate this fact, this article is hereby marked "advertisement" in accordance with 18 USC section 1734. This work is partly sponsored by grants from the National Key Basic Research Program of China (2013CB329506), National Science Foundation of China (NSFC) (no. 30900439, 30870834, 81101023, 81173468, 81271601), Ministry of Science and Technology of China (2012BAI13B06), and National Key Technology R&D Program (2012BAI01B08), Zhejiang Provincial Natural Science Foundation of China (LS13H18001), Fundamental Research Funds for the Central Universities, and by the China Postdoctoral Science Foundation. No other potential conflict of interest relevant to this article was reported.

ACKNOWLEDGMENT

We thank Cynthia Banks for editing of this manuscript.

REFERENCES

1. Bush G, Valera EM, Seidman LJ. Functional neuroimaging of attention-deficit/hyperactivity disorder: a review and suggested future directions. *Biol Psychiatry.* 2005;57:1273–1284.
2. Jones T, Rabiner EA. The development, past achievements, and future directions of brain PET. *J Cereb Blood Flow Metab.* 2012;32:1426–1454.
3. Nugent AC, Milham MP, Bain EE, et al. Cortical abnormalities in bipolar disorder investigated with MRI and voxel-based morphometry. *Neuroimage.* 2006;30:485–497.

4. Small GW, Bookheimer SY, Thompson PM, et al. Current and future uses of neuroimaging for cognitively impaired patients. *Lancet Neurol.* 2008;7: 161–172.
5. Kornblum HI, Araujo DM, Annala AJ, Tatsukawa KJ, Phelps ME, Cherry SR. In vivo imaging of neuronal activation and plasticity in the rat brain by high resolution positron emission tomography (microPET). *Nat Biotechnol.* 2000;18: 655–660.
6. Endepols H, Sommer S, Backes H, Wiedermann D, Graf R, Hauber W. Effort-based decision making in the rat: an [^{18}F]fluorodeoxyglucose micro positron emission tomography study. *J Neurosci.* 2010;30:9708–9714.
7. Bari A, Dalley JW, Robbins TW. The application of the 5-choice serial reaction time task for the assessment of visual attentional processes and impulse control in rats. *Nat Protoc.* 2008;3:759–767.
8. Robbins TW. The 5-choice serial reaction time task: behavioural pharmacology and functional neurochemistry. *Psychopharmacology (Berl).* 2002;163:362–380.
9. Nie B, Chen K, Zhao S, et al. A rat brain MRI template with digital stereotaxic atlas of fine anatomical delineations in paxinos space and its automated application in voxel-wise analysis. *Hum Brain Mapp.* 2013;34:1306–1318.
10. Pothuizen HH, Davies M, Aggleton JP, Vann SD. Effects of selective granular retrosplenial cortex lesions on spatial working memory in rats. *Behav Brain Res.* 2010;208:566–575.
11. Vann SD, Aggleton JP, Maguire EA. What does the retrosplenial cortex do? *Nat Rev Neurosci.* 2009;10:792–802.
12. Mesulam MM, Nobre AC, Kim YH, Parrish TB, Gitelman DR. Heterogeneity of cingulate contributions to spatial attention. *Neuroimage.* 2001;13:1065–1072.
13. Ahveninen J, Jaaskelainen IP, Belliveau JW, Hamalainen M, Lin FH, Raij T. Dissociable influences of auditory object vs. spatial attention on visual system oscillatory activity. *PLoS ONE.* 2012;7:e38511.
14. Mitelman SA, Shihabuddin L, Brickman AM, Hazlett EA, Buchsbaum MS. Volume of the cingulate and outcome in schizophrenia. *Schizophr Res.* 2005; 72:91–108.
15. Minoshima S, Giordani B, Berent S, Frey KA, Foster NL, Kuhl DE. Metabolic reduction in the posterior cingulate cortex in very early Alzheimer's disease. *Ann Neurol.* 1997;42:85–94.
16. Su YY, Luo B, Jin Y, et al. Altered neuronal intrinsic properties and reduced synaptic transmission of the rat's medial geniculate body in salicylate-induced tinnitus. *PLoS ONE.* 2012;7:e46969.
17. Mozolic JL, Joyner D, Hugenschmidt CE, et al. Cross-modal deactivations during modality-specific selective attention. *BMC Neurol.* 2008;8:35–45.
18. Elmquist JK, Elias CF, Saper CB. From lesions to leptin: hypothalamic control of food intake and body weight. *Neuron.* 1999;22:221–232.
19. Petrovich GD. Learning and the motivation to eat: forebrain circuitry. *Physiol Behav.* 2011;104:582–589.
20. Joseph MH, Datla K, Young AM. The interpretation of the measurement of nucleus accumbens dopamine by in vivo dialysis: the kick, the craving or the cognition? *Neurosci Biobehav Rev.* 2003;27:527–541.